Available online at www.sciencedirect.com

ScienceDirect

Journal of the Franklin Institute 359 (2022) 5712–5732

www.elsevier.com/locate/jfranklin

Functional interval estimation method for discrete-time switched systems under asynchronous switching

Jun Huang[a,*], Haochi Che[b], Hieu Trinh[c], Xudong Zhao[d], Yueyuan Zhang[a]

[a] *School of Mechanical and Electrical Engineering, Soochow University, Suzhou 215021, China*
[b] *School of Automation Science and Electrical Engineering, Beihang University, Beijing 100089, China*
[c] *School of Engineering, Deakin University, Geelong, VIC 3217, Australia*
[d] *School of Control Science and Engineering, Dalian University of Technology, Dalian 1160240, China*

Received 7 December 2021; received in revised form 12 April 2022; accepted 28 May 2022
Available online 4 June 2022

Abstract

This paper considers the issue of functional interval estimation in asynchronously discrete-time switched systems. Based on the H_∞ formalism, a functional observer is first proposed and a weighted attenuation performance is achieved. Then, reachability analysis is used to estimate its boundaries. Moreover, by comparing with the zonotope-based method, it is found that the proposed method can effectively reduce the conservatism caused by the reduction-order operation in zonotope-based method. Both methods are applied to a circuit system for the comparison purpose and to highlight the effectiveness of our results.

1. Introduction

The recent decades have witnessed extensive results in switched systems, which can model different kinds of practical engineering systems. The acquisition of accurate information of state variables is an important way to ensure the feasibility and reliability of the subsequent control process [1–3]. To investigate the stability of switched systems, a common Lyapunov

* Corresponding author.
E-mail address: cauchyhot@163.com (J. Huang).

https://doi.org/10.1016/j.jfranklin.2022.05.050

function (LF) was used to derive sufficient conditions for global asymptotic stability [4]. However, the common LF selected for the stability analysis in aforementioned work often resulted in restrictive conditions. In view of this, a multiple LF was considered [5]. Besides, to further guarantee stability of switched systems, the index of permissible commutation rates, such as average dwell time (ADT), was also considered [6]. In fact, the switching signals of the controllers or observers often cannot completely match the switching signals of original systems, so the existence of asynchronous switching (AS) is inevitable. Therefore, the synthesis problem with AS periods has been widely studied in recent years [7–10]. However, in these results, the considered LFs are required to be non-increasing during the running time of subsystems. Zhang and Shi [11] presented an extension that allows the increase of the partial LF during with the bounded increase rate. Besides, in view of the impact of switches between subsystems, a weighted disturbance attenuation (WDA) result needs to be given [12].

The interval observer (IO) is a powerful tool that can estimate the systems with uncertain terms [13]. For switched systems, the synchronous IO observer design methods have been studied in the references such as Marouani et al. [14], Garbouj et al. [15]. Recently, the design problem of IOs for switched systems using AS schemes has received significant research attention, but only a few results are available so far. The contradiction that its stability and positivity can not be satisfied at the same time has become a difficult problem in designing IOs. To solve the problem that the error systems can not satisfy the conditions imposed on both asymptotic stability and positivity, a novel type of IO structure was proposed, that is, the combination of set membership estimation (SME) method and H_∞ technique [16]. Observer gains obtained through H_∞ formalism can provide more freedom of design [17,18]. Meanwhile, the SME method (also known as deterministic method) uses geometric bodies (such as ellipsoids [19,20] and zonotopes [21,22]) to describe uncertainties and then constructs feasible sets to wrap all the required states to be estimated. The advantages of zonotope method over other geometric shapes lie in its less interval estimation conservatism and lower computational complexity, and it has recently attracted significant research interests [23–26]. In the work of Huang et al. [27], the zonotope-based method was used for the first time to design IOs for switched systems with AS periods. However, the implementation of the zonotope-based method relies on the usage of reduction-order operation to make the original zonotope wrapped in a new zonotope with fixed dimension, and it may lead to some conservatism on account of the wrapping effect [28]. To solve this probelm, an estimation method based on reachability analysis (RA) was proposed in Tang et al. [29].

Because of their potential to reduce the complexity and cost of design [30], functional observers (FOs) have received considerable research attention [31–33]. In the work of Emami et al. [31], a FO was designed for fault estimation, which is an important application of FOs. A solution to the problem of designing a minimum-order linear FO for time-invariant systems was presented in the work of Fernando et al. [32]. A simple way to check the functional observability before designing a FO was given in Jennings et al. [33]. In the context of functional interval observer (FIO), the recent works can be found in Gu et al. [34], Che et al. [35]. Gu et al. designed the first FIO for linear continuous-time systems [34]. Then, Che et al. [35] further improved design conditions and estimation accuracy in the work of Gu et al. [34]. Whereas, the method proposed in Che et al. [35] was based on zonotope, and the conservatism brought by its reduction operation has not been taken into account. A novel distributed FIO designed method was developed for nonlinear interconnected systems in the work of Huong et al. [36], which is the most recent study on distributed FIO. However, the problem of designing FIOs for switched systems under AS has still not been reported in the literature.

Thus, this paper presents a novel interval estimation method for discrete-time switched systems (DSSs) under AS. First, a robust FO with AS periods is designed and a reasonable WDA level is achieved. After that, the designed FO is combined with RA technique to recover the boundaries of DSSs. Moreover, the relationships and comparisons between the zonotope method and RA technique are discussed in detail. The contributions of this paper are threefold:

- By using the extended LF, a FO is first presented using the H_∞ formalism and a reasonable WDA level is achieved; and then, a FIO design method is presented for DSSs under AS.
- The conservatism brought by the zonotopic SME method is reduced by RA technique, and the interval estimation is more accurate. Furthermore, the superiority of RA technique is proved in theory and the comparison result is illustrated in the simulation.
- Compared with the traditional IO design method, the structures of the FIO designed by using the zonotopic method and RA technique do not require the error systems to be positive, which relax the design conditions of IO.

Different from Huang et al. [23], the asynchronous FIO design method for switched systems is considered in this paper. Compared with [27] that only considered the completely asynchronous case, this paper further considers the case that the switching signal of the system is partly asynchronous with the switching signal of the observer, which is a more general case of AS in practice. Besides, the RA technique is used and more tight bound is obtained in this paper.

This paper is structured as follows: Section 2 presents some preliminaries. Section 3 introduces an H_∞ FO for DSSs and then the bounds of the states are recovered by the zonotope method and RA technique, respectively. Then, the relationships between the two methods are discussed in detail in Section 4. Finally, Section 5 presents an example, where comparisons of the two mentioned methods are given and their performance is illustrated.

2. System description and preliminary

The symbols $>$, $\geq$, $<$ and $\leq$ should be understood elementwise. The matrix $A \prec 0$ ($\succ 0$), with $A^T = A \in \Re^{n\times n}$ defines that A is a negative (positive) definite matrix. $\overline{1,\alpha}$ stands for the sequence of integers $1,\ldots,\alpha$. $\overline{\lambda}(A)$ and $\underline{\lambda}(A)$ represent the largest and the smallest real part of the eigenvalues of matrix A, respectively.

A μ-dimensional zonotope $\aleph$ is denoted as $\aleph = \langle \eta, P\rangle = \eta \oplus P\mathbb{B}^\iota = \{\eta + Pz, z \in \mathbb{B}^\iota\}$, where $\eta \in \Re^\mu$ stands for the center of $\aleph$, $P \in \Re^{\mu\times\iota}$ stands for the generating matrix, $\mathbb{B}^\iota = [-1, 1]^\iota$ represents a hypercube, and $\oplus$ is Minkowski sum. The calculation of zonotope can be realized by Minkowski sum $\oplus$ and linear mapping $\odot$, i.e.,

$$\langle \eta_1, P_1\rangle \oplus \langle \eta_2, P_2\rangle = \langle \eta_1 + \eta_2, [P_1 \;\; P_2]\rangle,$$
$$F \odot \langle \eta, P\rangle = \langle F\eta, FP\rangle,$$

where $\eta,\ \eta_1,\ \eta_2 \in \Re^\mu$, $P,\ P_1,\ P_2 \in \Re^{\mu\times\iota}$, $F \in \Re^{l\times\mu}$ are known vectors and matrices.

Remark 2.1. The initial values of the state vector and the disturbance are enclosed by the following zonotopes:

$$z \in \zeta = \langle z_0, P\rangle,$$
$$u \in \Omega = \langle u_0, U\rangle,$$

where z_0, u_0 are known vectors, and P, U are given matrices.

Remark 2.2. To solve the problem that the dimension of zonotope continues to increase in the above calculations, a reduced-order operation that zonotope can be wrapped by fixed-dimensional zonotope is presented in Alamo et al. [21].

Interval vector (IV) $\mathcal{I}$ is denoted by $\mathcal{I} = [\phi, \varphi] = \{x : x \in \Re^{\mu}, \phi_r \le x_r \le \varphi_r, r \in \overline{1, \mu}\}$, where $\phi = [\phi_1, \dots, \phi_\mu]^T$, and $\varphi = [\varphi_1, \dots, \varphi_\mu]^T$.

Property 1. *For IVs* $[\phi, \varphi] \subset \Re^{\mu}$, $[\alpha, \varrho] \subset \Re^{\mu}$, *then,*

$$[\phi, \varphi] \oplus [\alpha, \varrho] = [\phi + \alpha, \varphi + \varrho].$$

Given a set of IVs,

$$\bigoplus_{r=1}^{m} \mathcal{I}_r = \mathcal{I}_1 \oplus \mathcal{I}_2 \dots \oplus \mathcal{I}_m.$$

The interval hull (IH) of a zonotope $\aleph$ is the smallest the IV that contains $\aleph$ (i.e., for a zonotope $\aleph = \langle \eta, P \rangle$, $\square(\aleph) = \{x : |x_r - \eta_r| \le ||P_r||_1, r \in \overline{1, \mu}\}$,)

Lemma 2.1 ([16]). *For a zonotope* $\aleph = \langle \eta, P \rangle$. *Its IH is given by*

$$\square(\aleph) = [\phi, \varphi],$$

where

$$\begin{cases} \phi_r = \eta_r - \sum_{s=1}^{\iota} |P_{r,s}|, \ \ r \in \overline{1, \mu}, \\ \varphi_r = \eta_r + \sum_{s=1}^{\iota} |P_{r,s}|, \ \ r \in \overline{1, \mu}. \end{cases}$$

Property 2. *Given the sets* $\aleph_i \subset \Re^{\mu}$, $i \in \overline{1, m}$,

$$\square\left(\bigoplus_{i=1}^{m} \aleph_i\right) = \bigoplus_{i=1}^{m} \square(\aleph_i).$$

The following DSS is considered:

$$\begin{cases} x(k+1) = A_{\sigma(k)}x(k) + B_{\sigma(k)}\omega(k), \\ y(k) = C_{\sigma(k)}x(k) + D_{\sigma(k)}f(k), \end{cases} \tag{1}$$

where $x(k) \in \Re^n$, $y(k) \in \Re^q$ are the state and output, respectively. $\omega(k) \in \Re^p$ and $f(k) \in \Re^m$ are the unknown but bounded disturbance and observation noise, respectively. $\sigma(k) : [0, \infty) \to \mathbb{S} = \{1, 2, \dots, N\}$ is the switching signal of the system. $A_i \in \Re^{n \times n}$, $B_i \in \Re^{n \times p}$, $C_i \in \Re^{q \times n}$ and $D_i \in \Re^{q \times m}$ $(i = \sigma(k) \in \mathbb{S})$ are constant matrices. For simplicity, k is omitted whenever necessary. When $i \in \mathbb{S}$, the estimated object is denoted by

$$\xi = F_i x, \tag{2}$$

where $F_i \in R^{\mu \times n}$ stands for a constant matrix. The purpose of this paper is to develop a frame $\{\underline{\xi}, \ \overline{\xi}\}$, which enables $\underline{\xi} \le \xi \le \overline{\xi}$, for any $k > 0$. Our first goal is to achieve an approximation $\hat{\xi}$ of function ξ by the following H_∞ FO:

$$\begin{cases} \hat{x}(k+1) = A_{\hat{\sigma}}\hat{x}(k) + L_{\hat{\sigma}}(y(k) - C_{\hat{\sigma}}\hat{x}(k)), \\ \hat{\xi}(k) = F_{\hat{\sigma}}\hat{x}(k), \end{cases} \tag{3}$$

where $\hat{\sigma} : [0, \infty) \to \mathbb{S} = \{1, 2, \dots, N\}$ is the observer signal, $A_j \in \Re^{n \times n}$, $C_j \in \Re^{q \times n}$ and $F_j \in \Re^{\mu \times n}$ $(\hat{\sigma} = j \in \mathbb{S})$ are constant matrices, and $L_j \in \Re^{n \times q}$ will be determined later. Let $e(k) =$

$x(k) - \hat{x}(k)$, then the error dynamic is

$$
\begin{aligned}
e(k+1) = {} & (A_j - L_jC_j)e + B_i\omega - L_jD_if \\
& + (A_i - A_j + L_jC_j - L_jC_i)x.
\end{aligned} \tag{4}
$$

Denote $z = [x^T \;\; e^T]^T$ and $u = [\omega^T \;\; f^T]^T$, the error dynamic (4) can be rewritten as

(i) $i = j$,

$$z(k+1) = \bar{A}_iz(k) + \bar{B}_iu(k), \tag{5}$$

where $\bar{A}_i = \begin{bmatrix} A_i & 0 \\ 0 & A_i - L_iC_i \end{bmatrix}$, and $\bar{B}_i = \begin{bmatrix} B_i & 0 \\ B_i & -L_iD_i \end{bmatrix}$. Then, the estimation error can be formulated as

$$
\begin{aligned}
\delta(k+1) &= F_ix(k+1) - F_i\hat{x}(k+1) \\
&= (F_i - F_i)x(k+1) + F_ie(k+1) \\
&= \bar{\Theta}_iz(k+1) \\
&= \bar{\Theta}_i\bar{A}_iz + \bar{\Theta}_i\bar{B}_iu,
\end{aligned} \tag{6}
$$

where $\bar{\Theta}_i = [0 \;\; F_i]$.

(ii) $i \neq j$

$$z(k+1) = \tilde{A}_iz(k) + \tilde{B}_iu(k), \tag{7}$$

where

$$\tilde{A}_i = \begin{bmatrix} A_i & 0 \\ A_i - A_j + L_jC_j - L_jC_i & A_j - L_jC_j \end{bmatrix},$$

$$\tilde{B}_i = \begin{bmatrix} B_i & 0 \\ B_i & -L_jD_i \end{bmatrix}.$$

Similarly, we can get

$$
\begin{aligned}
\delta(k+1) &= F_ix(k+1) - F_j\hat{x}(k+1) \\
&= (F_i - F_j)x(k+1) + F_je(k+1) \\
&= \tilde{\Theta}_iz(k+1) \\
&= \tilde{\Theta}_i\tilde{A}_iz + \tilde{\Theta}_i\tilde{B}_iu,
\end{aligned} \tag{8}
$$

where $\tilde{\Theta}_i = [F_i - F_j \;\; F_j]$.

Definition 2.1 ([7]). Observer (3) is known as the H_∞ FO, if

(1) $u = 0$, then the errors (6) and (8) satisfy asymptotic stablity;
(2) $u \neq 0$, for $\delta(0) = 0$, we have

$$\sum_{k=0}^{\infty} \delta^T\delta < \gamma \sum_{k=0}^{\infty} u^Tu,$$

where $\gamma > 0$ is the disturbance attenuation (DA) level.

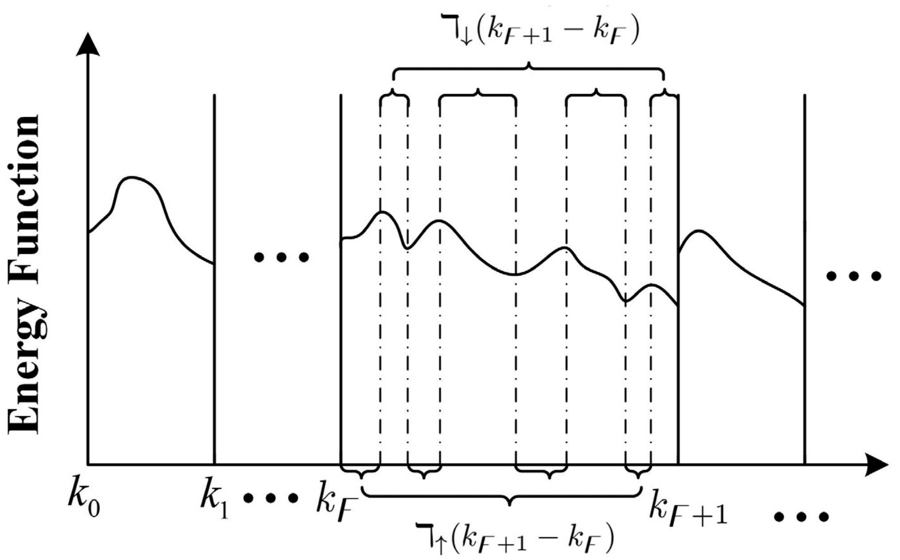

Fig. 1. Extended LF.

Definition 2.2 ([27])**.** For interval $[k_1, k_2)$ and $k_1 \geq 0$, $N_\sigma(k_1, k_2)$ is defined as switching number of switching signal σ on $[k_1, k_2)$. If

$$N_\sigma(k_1, k_2) \leq N_0 + \frac{(k_2 - k_1)}{\tau^*},$$

where $N_0 \geq 0$ and $\tau^* > 0$, then τ^* is an ADT of σ. In this paper, let $N_0 = 0$.

Considering the influence of switching among subsystems, the improved Definition 1 is obtained and a WDA result is given.

Definition 2.3 ([12])**.** Observer (3) is known as an H_∞ FO for DSS (1), if

(1) $u = 0$, then the errors (6) and (8) satisfy asymptotic stability;
(2) $u \neq 0$, for $\delta(0) = 0$, we have

$$\sum_{k=0}^{\infty} \kappa \delta^T \delta < \gamma \sum_{k=0}^{\infty} u^T u,$$

where $\gamma > 0$ is the WDA level and $0 < \kappa < 1$ is given constant.

Remark 2.3. To improve the previous results in Xiang et al. [7], Huang et al. [27], a class of LFs allowed to increase with bounded increase rate are illustrated in Fig. 1. As shown, for interval $[k_F, k_{F+1})$, $\forall F \in \mathbb{S}$, we denote $\urcorner_{\uparrow}(k_F, k_{F+1})$ and $\urcorner_{\downarrow}(k_F, k_{F+1})$ as the sets of the scattered intervals that LF is increasing and decreasing within the interval $[k_F, k_{F+1})$, i.e., we have $[k_F, k_{F+1}) := \urcorner_{\downarrow}(k_F, k_{F+1}) \cup \urcorner_{\uparrow}(k_F, k_{F+1})$. In addition, the length of $\urcorner_{\downarrow}(k_F, k_{F+1})$ and $\urcorner_{\uparrow}(k_F, k_{F+1})$ is defined as $\urcorner_{\downarrow}(k_{F+1} - k_F)$ and $\urcorner_{\uparrow}(k_{F+1} - k_F)$, respectively.

Remark 2.4. In order to investigate the issue of AS, the case that the period $\urcorner_{\uparrow}(k_F, k_{F+1})$ is the only interval close to the switching instants as illustrated in Fig. 2 is considered and we

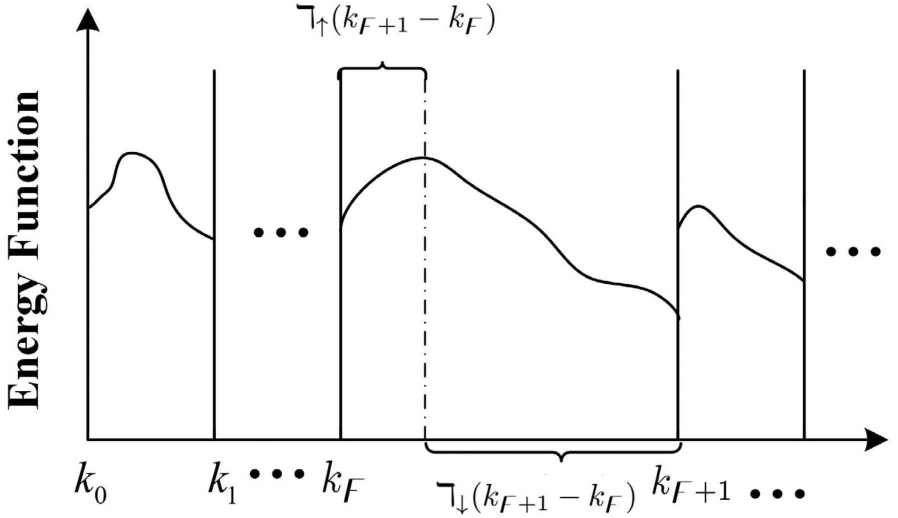

Fig. 2. Typical case of the extended LF.

denote $\daleth_M = \max_{F\in\mathbb{S}} \daleth_{\uparrow}(k_{F+1}-k_F)$. In addition, the delay of AS is also assumed to be $\daleth_M$. For $k \in [k_F, k_F+\daleth_M)$, we know $\hat{\sigma}(k) = \sigma(k-\daleth_M) = j$, $\sigma(k) = i$, $i \neq j$, then according to the above discussion, we have

$$z(k+1) = \tilde{A}_i z(k) + \tilde{B}_i u(k). \qquad \forall k \in [k_F, k_F+\daleth_M)$$

Similarly, for $k \in [k_F+\daleth_M, k_{F+1})$, we have $\hat{\sigma}(k) = \sigma(k-\daleth_M) = i$, $\sigma(k) = i$ and the error dynamic is given by

$$z(k+1) = \bar{A}_i z(k) + \bar{B}_i u(k). \qquad \forall k \in [k_F+\daleth_M, k_{F+1})$$

The proof of the normal situation can be completed by the same technique and ideas in the above case.

3. Main result

In this section, sufficient conditions for the existence of the observer (3) are given, and then the zonotopic SME method in Huang et al. [27] is extended to construct the FIO. After that, a novel estimation method is proposed for the design of FIO.

Theorem 3.1. *Given scalars $0 < \alpha < 1$, $\beta \geq 0$ and $\pi > 1$. Supposed that there are a constant $\gamma > 0$, block-diagonal matrices $\Xi_i = \Xi_i^T$, $\Xi_j = \Xi_j^T \in \Re^{2n\times 2n} \succ 0$, $R_i \in \Re^{n\times q}$ and $R_j \in \Re^{n\times q}$ such that for any $(\sigma(k_F) = i,\ \sigma(k_F-1) = j) \in \mathbb{S}$, $j \neq i$*

$$\begin{bmatrix} \Gamma_1 & * & * & * & * \\ 0 & \Phi_1 & * & * & * \\ B_i^T G_i A_i & \Pi_1 & \Sigma_1 & * & * \\ 0 & 0 & -D_i^T R_i^T B_i & -\gamma I & * \\ 0 & \Lambda_1^T & 0 & -R_i D_i & -H_i \end{bmatrix} \prec 0, \tag{9}$$

$$\begin{bmatrix} \Gamma_2 & * & * & * & * \\ \Pi_2 & \Phi_2 & * & * & * \\ B_i^T G_i A_i & 0 & B_i^T G_i B_i - \gamma I & * & * \\ 0 & 0 & 0 & -\gamma I & * \\ \Sigma_2^T & \Lambda_2^T & H_i B_i & -R_j D_i & -H_i \end{bmatrix} \prec 0, \tag{10}$$

and

$$\Xi_i \prec \pi \Xi_j, \tag{11}$$

with an ADT satisfying

$$\tau^* > -\frac{\daleth_M \ln\theta + \ln\pi}{\ln(1-\alpha)}, \tag{12}$$

then, Eq. (3) is an H_∞ FO of system (1) and a WDA level γ is achieved, where

$$\theta = \frac{(1+\beta)}{(1-\alpha)}, \quad \Xi_i = \begin{bmatrix} G_i & 0 \\ 0 & H_i \end{bmatrix}, \quad \Xi_j = \begin{bmatrix} G_j & 0 \\ 0 & H_j \end{bmatrix},$$

$$\Gamma_1 = A_i^T G_i A_i + \alpha G_i - G_i,$$

$$\Pi_1 = B_i^T H_i A_i - B_i^T R_i C_i,$$

$$\Phi_1 = \alpha H_i - H_i + F_i^T F_i,$$

$$\Sigma_1 = B_i^T G_i B_i + B_i^T H_i B_i - \gamma I,$$

$$\Lambda_1 = A_i^T H_i^T - C_i^T R_i^T,$$

$$\Gamma_2 = A_i^T G_i A_i - \beta G_i - G_i + (F_i - F_j)^T (F_i - F j),$$

$$\Pi_2 = F_j^T (F_i - F j),$$

$$\Phi_2 = -\beta H_i - H_i + F_j^T F_j,$$

$$\Sigma_2 = A_i^T H_i^T - A_j^T H_i^T + C_j^T R_j^T - C_i^T R_j^T,$$

$$\Lambda_2 = A_j^T H_i^T - C_j^T R_j^T,$$

and the gains L_i and L_j are determined by $L_i = (H_i)^{-1} R_i$ and $L_j = (H_i)^{-1} R_j$, respectively. After that, we can further obtain the optimal observer by the following operation

$$\min \quad \gamma \qquad s.t. \quad (9) - (12).$$

Proof. Substitute $R_i = H_i L_i$ into (9), then we rewrite (9) as follows:

$$\Psi = \begin{bmatrix} \Psi_{11} & \Psi_{12} \\ \Psi_{12}^T & \Psi_{22} \end{bmatrix} \prec 0,$$

where

$$\Psi_{11} = \begin{bmatrix} \Gamma_1 & * & * & * \\ 0 & \Phi_1 & * & * \\ B_i^T G_i A_i & \Pi_1 & \Sigma_1 & * \\ 0 & 0 & -D_i^T R_i^T B_i & -\gamma I \end{bmatrix},$$

$$\Psi_{12} = \begin{bmatrix} 0 \\ \Lambda_1 \\ 0 \\ -D_i^T L_i^T H_i^T \end{bmatrix}, \quad \Psi_{22} = -H_i.$$

Since $\Psi_{22} \prec 0$, using Schur complement [37], we have

$\Psi_{11} - \Psi_{12}\Psi_{22}^{-1}\Psi_{12}^T \prec 0,$

thus,

$$\begin{bmatrix} \bar{A}_i^T \Xi_i \bar{A}_i + \alpha \Xi_i - \Xi_i + \bar{\Theta}_i^T \bar{\Theta}_i & * \\ \bar{B}_i^T \Xi_i \bar{A}_i & \bar{B}_i^T \Xi_i \bar{B}_i - \gamma I \end{bmatrix} \prec 0. \tag{13}$$

Similarly, (10) can be rewritten as

$$\begin{bmatrix} \tilde{A}_i^T \Xi_i \tilde{A}_i - \beta \Xi_i - \Xi_i + \tilde{\Theta}_i^T \tilde{\Theta}_i & * \\ \tilde{B}_i^T \Xi_i \tilde{A}_i & \tilde{B}_i^T \Xi_i \tilde{B}_i - \gamma I \end{bmatrix} \prec 0. \tag{14}$$

At first, let $u = 0$. Consider the following multiple LF

$V_i = z^T \Xi_i z, \quad i \in \mathbb{S}.$

For $k \in [k_F, k_F + \urcorner_M)$, we know $\hat{\sigma} = \sigma(k - \urcorner_M) = j$ and $\sigma(k) = i$. Taking the forward difference of $V_i(k)$ yields

$$\begin{aligned} \Delta V_i(k) &= V_i(k+1) - V_i(k) \\ &= z^T (\tilde{A}_i^T \Xi_i \tilde{A}_i - \Xi_i) z. \end{aligned}$$

The inequality (14) implies that $\tilde{A}_i^T \Xi_i \tilde{A}_i - \beta \Xi_i - \Xi_i + \tilde{\Theta}_i^T \tilde{\Theta}_i \prec 0$, then,

$$\begin{aligned} \Delta V_i(k) &< \beta V_i(k) - z^T \tilde{\Theta}_i^T \tilde{\Theta}_i z \\ &< \beta V_i(k). \end{aligned}$$

Analogously, for $k \in [k_F + \urcorner_M, k_{F+1})$, from (13) we deduce

$$\begin{aligned} \Delta V_i(k) &< -\alpha V_i(k) - z^T \bar{\Theta}_i^T \bar{\Theta}_i z \\ &< -\alpha V_i(k). \end{aligned}$$

By sorting out the above contents and combining with Remark 2.4, we can get

$$\begin{cases} \Delta V_i(k) < \beta V_i(k), & \forall k \in \urcorner_\uparrow(k_F, k_{F+1}) \\ \Delta V_i(k) < -\alpha V_i(k). & \forall k \in \urcorner_\downarrow(k_F, k_{F+1}) \end{cases} \tag{15}$$

For $\forall k \in [k_F, k_{F+1})$, it holds from (15) that

$$\begin{aligned} V_i(k) &< (1-\alpha)^{\urcorner_\downarrow(k-k_F)}(1+\beta)^{\urcorner_\uparrow(k-k_F)} V_i(k_F) \\ &< (1-\alpha)^{[\urcorner_\downarrow(k-k_F)+\urcorner_\uparrow(k-k_F)]}\theta^{\urcorner_\uparrow(k-k_F)} V_i(k_F) \\ &< (1-\alpha)^{(k-k_F)}\theta^{\urcorner_\uparrow(k-k_F)} V_i(k_F). \end{aligned} \tag{16}$$

Then, by inequality (11), the following inequality can be derived

$$V_i(k) < (1-\alpha)^{(k-k_F)}\theta^{\urcorner_\uparrow(k-k_F)}\pi V_j(k_F). \tag{17}$$

Repeating (16) and (17), we can conclude

$$V_{\sigma(k)}(k) < (1-\alpha)^k (\theta^{\urcorner_M})^{N_\sigma(0,k)} \pi^{N_\sigma(0,k)} V_{\sigma(0)}(0). \tag{18}$$

Since $N_\sigma(0,k) \le \dfrac{k}{\tau^*}$, and substituting it into (18), then

$$V_{\sigma(k)}(k) < [(1-\alpha)\theta^{\frac{\urcorner_M}{\tau^*}}\pi^{\frac{1}{\tau^*}}]^k V_{\sigma(0)}(0).$$

Due to $V_{\sigma(0)}(0) \le \overline{\lambda}(\Xi_{\sigma(0)})||z(0)||^2$ and $V_{\sigma(k)}(k) \ge \underline{\lambda}(\Xi_{\sigma(k)})||z(k)||^2$, we have

$$||z(k)|| < \sqrt{\frac{\overline{\lambda}(\Xi_{\sigma(0)})[(1-\alpha)\theta^{\frac{\urcorner_M}{\tau^*}}\pi^{\frac{1}{\tau^*}}]^k}{\underline{\lambda}(\Xi_{\sigma(k)})}}||z(0)||.$$

Given (12), we can get

$$\begin{aligned}(1-\alpha)\theta^{\frac{\urcorner_M}{\tau^*}}\pi^{\frac{1}{\tau^*}} &< (1-\alpha)\theta^{(\frac{-\urcorner_M \ln(1-\alpha)}{\urcorner_M \ln\theta+\ln\pi})}\pi^{(\frac{-\ln(1-\alpha)}{\urcorner_M \ln\theta+\ln\pi})} \\ &< (1-\alpha)(\theta^{\urcorner_M}\pi)^{(\frac{-\ln(1-\alpha)}{\urcorner_M \ln\theta+\ln\pi})} \\ &< (1-\alpha)(e^{\urcorner_M \ln\theta+\ln\pi})^{(\frac{-\ln(1-\alpha)}{\urcorner_M \ln\theta+\ln\pi})} \\ &< \frac{1-\alpha}{1-\alpha} = 1,\end{aligned}$$

that is

$$\lim_{k\to+\infty}||z(k)|| = \lim_{k\to+\infty}\sqrt{\frac{\overline{\lambda}(\Xi_{\sigma(0)})[(1-\alpha)\theta^{\frac{\urcorner_M}{\tau^*}}\pi^{\frac{1}{\tau^*}}]^k}{\underline{\lambda}(\Xi_{\sigma(k)})}}||z(0)|| = 0.$$

Due to

$$\begin{cases} ||\delta(k)|| < ||\tilde{\Theta}_i|| \cdot ||z(k)||, & \forall k \in \urcorner_{\uparrow}(k_F, k_{F+1}) \\ ||\delta(k)|| < ||\tilde{\Theta}_i|| \cdot ||z(k)||, & \forall k \in \urcorner_{\downarrow}(k_F, k_{F+1}) \end{cases}$$

thus, it is obvious that

$$\lim_{k\to+\infty}||\delta(k)|| = 0.$$

Therefore, the error $\delta(k)$ satisfies asymptotic stability when $u = 0$.

Now, consider $u \neq 0$. For $k \in [k_F, k_F + \urcorner_M)$, according to inequality (14), one can obtain

$$M^T\begin{bmatrix}\tilde{A}_i^T\Xi_i\tilde{A}_i - \beta\Xi_i - \Xi_i + \tilde{\Theta}_i^T\tilde{\Theta}_i & * \\ \tilde{B}_i^T\Xi_i\tilde{A}_i & \tilde{B}_i^T\Xi_i\tilde{B}_i - \gamma I\end{bmatrix}M < 0, \tag{19}$$

where $M = [z^T \quad u^T]^T$. In light of the derivation of (19), we have

$$z^T[\tilde{A}_i^T\Xi_i\tilde{A}_i - \beta\Xi_i - \Xi_i + \tilde{\Theta}_i^T\tilde{\Theta}_i]z + 2u^T\tilde{B}_i^T\Xi_i\tilde{A}_iz + u^T(\tilde{B}_i^T\Xi_i\tilde{B}_i - \gamma I)u < 0. \tag{20}$$

Further simplifying (20) yields

$$\Delta V_i - \beta V_i + \delta^T\delta - \gamma u^Tu < 0.$$

Analogously, according to inequality (13), for $k \in [k_F + \urcorner_M, k_{F+1})$, it yields

$$\Delta V_i + \alpha V_i + \delta^T\delta - \gamma u^Tu < 0.$$

Therefore, one has

$$\begin{cases} \Delta V_i < \beta V_i - \delta^T\delta + \gamma u^Tu, & \forall k \in \urcorner_{\uparrow}(k_F, k_{F+1}) \\ \Delta V_i < -\alpha V_i - \delta^T\delta + \gamma u^Tu. & \forall k \in \urcorner_{\downarrow}(k_F, k_{F+1}) \end{cases} \tag{21}$$

For $k \in [k_F, k_{F+1})$, we have

$$V_i(k) < (1-\alpha)^{(k-k_F)}\theta^{\urcorner_{\uparrow}(k-k_F)}V_i(k_F) - \sum_{\varsigma=k_F}^{k-1}(1-\alpha)^{k-\varsigma-1}\theta^{\urcorner_{\uparrow}[(k-1)-\varsigma]}T(\varsigma),$$

where $T(\varsigma) = \delta^T(\varsigma)\delta(\varsigma) - \gamma u^T(\varsigma)u(\varsigma)$. Since $\Xi_i \prec \pi\Xi_j$, it follows that

$$V_i(k) < (1-\alpha)^{(k-k_F)}\theta^{\daleth_\uparrow(k-k_F)}\pi V_j(k_F) - \sum_{\varsigma=k_F}^{k-1}(1-\alpha)^{k-\varsigma-1}\theta^{\daleth_\uparrow[(k-1)-\varsigma]}T(\varsigma). \tag{22}$$

Repeating (21) and (22), we get

$$\begin{aligned}V_i(k) &< \pi^{N_\sigma(0,k)}(1-\alpha)^k\theta^{\daleth_\uparrow(k-0)}V_{\sigma(0)}(0)\\ &\quad - \sum_{\varsigma=0}^{k-1}\pi^{N_\sigma(\varsigma,k)}(1-\alpha)^{k-\varsigma-1}\theta^{\daleth_\uparrow[(k-1)-\varsigma]}T(\varsigma).\end{aligned}$$

Denote that $V_{\sigma(0)}(0) = 0$, given $V_i(k) > 0$, then

$$\sum_{\varsigma=0}^{k-1}\pi^{N_\sigma(\varsigma,k)}(1-\alpha)^{k-\varsigma-1}\theta^{\daleth_\uparrow[(k-1)-\varsigma]}T(\varsigma) < 0. \tag{23}$$

Further simplifying (23) yields

$$\begin{aligned}&\sum_{\varsigma=0}^{k-1}\pi^{N_\sigma(\varsigma,k)}(1-\alpha)^{k-\varsigma-1}\theta^{\daleth_\uparrow[(k-1)-\varsigma]}\delta^T(\varsigma)\delta(\varsigma)\\ &\quad < \sum_{\varsigma=0}^{k-1}\pi^{N_\sigma(\varsigma,k)}(1-\alpha)^{k-\varsigma-1}\theta^{\daleth_\uparrow[(k-1)-\varsigma]}\gamma u^T(\varsigma)u(\varsigma).\end{aligned} \tag{24}$$

Multiplying both sides of the inequality (24) by $\pi^{-N_\sigma(0,k)}\theta^{-\daleth_\uparrow[(k-1)-0]}$, we can conclude

$$\begin{aligned}&\sum_{\varsigma=0}^{k-1}\pi^{-N_\sigma(0,\varsigma)}\theta^{-\daleth_\uparrow(\varsigma-0)}(1-\alpha)^{k-\varsigma-1}\delta^T(\varsigma)\delta(\varsigma)\\ &\quad < \sum_{\varsigma=0}^{k-1}\pi^{-N_\sigma(0,\varsigma)}\theta^{-\daleth_\uparrow(\varsigma-0)}(1-\alpha)^{k-\varsigma-1}\gamma u^T(\varsigma)u(\varsigma).\end{aligned}$$

By $\daleth_\uparrow(\varsigma-0) < \daleth_M N_\sigma(0,\varsigma)$ and $\pi^{-N_\sigma(0,\varsigma)}\theta^{-\daleth_\uparrow(\varsigma-0)} < 1$, the above inequality can be converted to

$$\sum_{\varsigma=0}^{k-1}\pi^{-N_\sigma(0,\varsigma)}\theta^{-\daleth_M N_\sigma(0,\varsigma)}(1-\alpha)^{k-\varsigma-1}\delta^T(\varsigma)\delta(\varsigma) < \sum_{\varsigma=0}^{k-1}(1-\alpha)^{k-\varsigma-1}\gamma u^T(\varsigma)u(\varsigma).$$

Given the definition of ADT, we have $N_\sigma(0,\varsigma) < \dfrac{\varsigma}{\tau^*}$, then

$$\sum_{\varsigma=0}^{k-1}\pi^{-\frac{\varsigma}{\tau^*}}\theta^{-\daleth_M\frac{\varsigma}{\tau^*}}(1-\alpha)^{k-\varsigma-1}\delta^T(\varsigma)\delta(\varsigma) < \sum_{\varsigma=0}^{k-1}(1-\alpha)^{k-\varsigma-1}\gamma u^T(\varsigma)u(\varsigma),$$

that is

$$\sum_{k=0}^{\infty}\sum_{\varsigma=0}^{k-1}\pi^{-\frac{\varsigma}{\tau^*}}\theta^{-\daleth_M\frac{\varsigma}{\tau^*}}(1-\alpha)^{k-\varsigma-1}\delta^T(\varsigma)\delta(\varsigma) < \sum_{k=0}^{\infty}\sum_{\varsigma=0}^{k-1}(1-\alpha)^{k-\varsigma-1}\gamma u^T(\varsigma)u(\varsigma). \tag{25}$$

Further simplifying (25), the following result is derived:

$$\begin{aligned} &\sum_{\varsigma=0}^{\infty}\sum_{k=\varsigma}^{\infty}\pi^{-\frac{\varsigma}{\tau^*}}\theta^{-\urcorner_M\frac{\varsigma}{\tau^*}}(1-\alpha)^{k-\varsigma-1}\delta^T(\varsigma)\delta(\varsigma) < \sum_{\varsigma=0}^{\infty}\sum_{k=\varsigma}^{\infty}(1-\alpha)^{k-\varsigma-1}\gamma u^T(\varsigma)u(\varsigma), \\ &\Leftrightarrow \sum_{\varsigma=0}^{\infty}\pi^{-\frac{\varsigma}{\tau^*}}\theta^{-\urcorner_M\frac{\varsigma}{\tau^*}}\delta^T(\varsigma)\delta(\varsigma)\sum_{k=\varsigma}^{\infty}(1-\alpha)^{k-\varsigma-1} < \sum_{\varsigma=0}^{\infty}\gamma u^T(\varsigma)u(\varsigma)\sum_{k=\varsigma}^{\infty}(1-\alpha)^{k-\varsigma-1}, \\ &\Leftrightarrow \sum_{\varsigma=0}^{\infty}\pi^{-\frac{\varsigma}{\tau^*}}\theta^{-\urcorner_M\frac{\varsigma}{\tau^*}}\delta^T(\varsigma)\delta(\varsigma) < \sum_{\varsigma=0}^{\infty}\gamma u^T(\varsigma)u(\varsigma). \end{aligned} \tag{26}$$

From (12), we can conclude

$$\begin{aligned} \pi^{-\frac{\varsigma}{\tau^*}}\theta^{-\urcorner_M\frac{\varsigma}{\tau^*}} &> \pi^{\left(\frac{\varsigma\ln(1-\alpha)}{\urcorner_M\ln\theta+\ln\pi}\right)}\theta^{\left(\frac{\urcorner_M\varsigma\ln(1-\alpha)}{\urcorner_M\ln\theta+\ln\pi}\right)} \\ &> (\theta^{\urcorner_M}\pi)^{\left(\frac{\varsigma\ln(1-\alpha)}{\urcorner_M\ln\theta+\ln\pi}\right)} \\ &> (e^{\urcorner_M\ln\theta+\ln\pi})^{\left(\frac{\varsigma\ln(1-\alpha)}{\urcorner_M\ln\theta+\ln\pi}\right)} \\ &> (1-\alpha)^{\varsigma}. \end{aligned} \tag{27}$$

By (26) and (27), it is obvious that

$$\sum_{\varsigma=0}^{\infty}(1-\alpha)^{\varsigma}\delta^T(\varsigma)\delta(\varsigma) < \sum_{\varsigma=0}^{\infty}\gamma u^T(\varsigma)u(\varsigma). \tag{28}$$

In view of the previous discussion, we can conclude that Eq. (3) is the H_∞ FO of system (1) and the error dynamics achieve a WDA level γ. □

Remark 3.1. Due to the existence of $(1-\alpha)^{\varsigma}$, the inequality (28) illustrates that the error dynamics achieve a WDA level from $u(\varsigma)$ to $\delta(\varsigma)$. When $\alpha = 0$, it means that there is no switching between subsystems, and (28) shrinks to normal DA for a single subsystem. When α is small enough, it means that ADT is given sufficiently large, obviously inequality (28) approaches the normal DA.

Remark 3.2. The energy function considered in Theorem 1 can increase during the running time of the subsystem, which relaxes the counterparts of previous works in Xiang et al. [7], Huang et al. [27].

3.1. Design of FIO by the zonotope method

Given H_∞ observer, a SME method based on zonotope is now extended to the design of FIO for DSSs with AS.

Proposition 3.1 ([27]). *Suppose $u \in \Omega = \langle 0, U\rangle$. The linear function $\xi = F_i x$ can be enclosed by the following zonotope*

$$\langle \hat{\xi},\ \Theta_i^* P\rangle,$$

where $\hat{\xi} = F_{\hat{\sigma}}\hat{x}$ is the estimation of ξ by (3), and $P \in R^{2n\times 2n}$ satisfies

$$P(k+1) = [A_i^*\hat{P}(k) \quad B_i^* U],$$

where $\hat{P}(k)$ is given by the reduced-order algorithm in Alamo et al. [21], A_i^*, Θ_i^* and B_i^* are the matrices that vary with the modes, and their values are given by

$$A_i^* = \begin{cases} \bar{A}_i, & \text{if } k \in \urcorner_\downarrow \\ \tilde{A}_i, & \text{if } k \in \urcorner_\uparrow \end{cases}$$

$$\Theta_i^* = \begin{cases} \bar{\Theta}_i, & \text{if } k \in \urcorner_\downarrow \\ \tilde{\Theta}_i, & \text{if } k \in \urcorner_\uparrow \end{cases}$$

and

$$B_i^* = \begin{cases} \bar{B}_i, & \text{if } k \in \urcorner_\downarrow \\ \tilde{B}_i. & \text{if } \ k \in \urcorner_\uparrow \end{cases}$$

Remark 3.3. Given Remark 2.1, we denote

$$z(k) \in \hat{\zeta}^z(k) = \big\langle 0, \ P(k) \big\rangle.$$

Then, we have

$$P(k+1) = [A_i^* \hat{P}(k) \quad B_i^* U]. \tag{29}$$

The proof process refers to the previous work [27]. Following the Eq. (8), it yields

$$\delta(k) \in \Theta_i^* \hat{\zeta}^z(k) = \big\langle 0, \ \Theta_i^* P(k) \big\rangle.$$

Since $\xi = \hat{\xi} + \delta$, we have

$$\xi(k) \in \big\langle \hat{\xi}(k), \ \Theta_i^* P(k) \big\rangle.$$

Remark 3.4. We define $\langle \hat{\xi}, \Theta_i^* P \rangle = \langle \hat{\xi}, \Upsilon \rangle$. Given Lemma 2.1, the following IV can be obtained

$$[\underline{\xi}^z, \overline{\xi}^z] = \square\big(\langle \hat{\xi}, \Upsilon \rangle\big),$$

where

$$\begin{cases} \overline{\xi}_r^{\,z} = \hat{\xi}_r + \sum_{s=1}^{\iota} |\Upsilon_{r,s}|, & r = 1, \ldots, \mu, \\ \underline{\xi}_r^{\,z} = \hat{\xi}_r - \sum_{s=1}^{\iota} |\Upsilon_{r,s}|, & r = 1, \ldots, \mu. \end{cases}$$

Thus, given the errors (6) and (8), there exists an IV $[\underline{\delta}^z, \overline{\delta}^z]$ such that $\underline{\delta}^z \leq \delta \leq \overline{\delta}^z$, then, we further have

$$\hat{\xi} + \underline{\delta}^z \leq \xi \leq \hat{\xi} + \overline{\delta}^z.$$

So, the FIO by zonotopic SME method can now be written as

$$\begin{cases} \overline{\xi}^z = \hat{\xi} + \overline{\delta}^z, \\ \underline{\xi}^z = \hat{\xi} + \underline{\delta}^z, \end{cases} \tag{30}$$

where

$$[\underline{\delta}^z, \overline{\delta}^z] = \square\big(\Theta_i^* \hat{\xi}^z\big) = \square\big(\langle 0, \Upsilon \rangle\big).$$

3.2. Design of FIO by the RA technique

In this part, the FIO based on Eq. (3) by RA technique is also derived by

$$\begin{cases} \overline{\xi}^h = \hat{\xi} + \overline{\delta}^h, \\ \underline{\xi}^h = \hat{\xi} + \underline{\delta}^h. \end{cases} \tag{31}$$

where $\underline{\delta}^h \leq \delta \leq \overline{\delta}^h$ and satisfies the following theorem.

Theorem 3.2. *Consider the observer (31) and take the same initial values as the zonotope method in Proposition 3.1, i.e.,*

Algorithm 1 Steps for FIO by the RA technique.

Require: $\hat{x}(0), P(0), U, F_j$

Ensure: $\underline{\xi}^h$, $\overline{\xi}^h$

1: **Begin:**
2: $\hat{x}(0) = x_0, z(0) \in \hat{\zeta}^z(0) = \langle 0, P(0)\rangle$, $u \in \Omega = \langle 0, U\rangle$;
3: **for** $k \geq 0$ **do**
4: $\quad \hat{x}(k+1) = A_{\hat{\sigma}}\hat{x}(k) + L_{\hat{\sigma}}(y(k) - C_{\hat{\sigma}}\hat{x}(k))$
5: $\quad \hat{\xi} = F_{\hat{\sigma}}\hat{x}$
6: $\quad \delta(k) = \Theta_i^*\big[(\bar{A}_i)^{\urcorner_\downarrow(k-0)}(\tilde{A}_i)^{\urcorner_\uparrow(k-0)}z(0) + \sum_{\varsigma=0}^{k-1}(\bar{A}_i)^{\urcorner_\downarrow[k-(\varsigma+1)]}(\tilde{A}_i)^{\urcorner_\uparrow[k-(\varsigma+1)]}B_i^{\diamond}u(\varsigma)\big]$
7: $\quad \hat{\zeta}^h(0) = \langle 0, \tilde{\Theta}_i P(0)\rangle$
8: $\quad \delta(0) \in \hat{\zeta}^h(0) \subseteq [\underline{\delta}^h(0), \overline{\delta}^h(0)] = \Box\big(\langle 0, \tilde{\Theta}_i P(0)\rangle\big)$
9: $\quad \delta(k) \in \hat{\zeta}^h(k) = \Theta_i^*\big[(\bar{A}_i)^{\urcorner_\downarrow(k-0)}(\tilde{A}_i)^{\urcorner_\uparrow(k-0)}\hat{\zeta}^z(0) \oplus \bigoplus_{\varsigma=0}^{k-1}(\bar{A}_i)^{\urcorner_\downarrow[k-(\varsigma+1)]}(\tilde{A}_i)^{\urcorner_\uparrow[k-(\varsigma+1)]}B_i^{\diamond}\langle 0, U\rangle\big]$
10: $\quad [\underline{\delta}^h, \overline{\delta}^h] = \Box\big(\Theta_i^*(\bar{A}_i)^{\urcorner_\downarrow(k-0)}(\tilde{A}_i)^{\urcorner_\uparrow(k-0)}\hat{\zeta}^z(0)\big) \oplus \bigoplus_{\varsigma=0}^{k-1}\Box\big(\Theta_i^*(\bar{A}_i)^{\urcorner_\downarrow[k-(\varsigma+1)]}(\tilde{A}_i)^{\urcorner_\uparrow[k-(\varsigma+1)]}B_i^{\diamond}\Omega\big)$
11: $\quad \overline{\xi}^h = \hat{\xi} + \overline{\delta}^h$
12: $\quad \underline{\xi}^h = \hat{\xi} + \underline{\delta}^h$;
13: **end for**

$$z(0) \in \hat{\zeta}^z(0) = \langle 0,\ P(0)\rangle, \tag{32}$$

$$u \in \Omega = \langle 0,\ U\rangle. \tag{33}$$

Then, the estimation object ξ is bounded by the interval vector $[\underline{\xi}^h,\ \overline{\xi}^h]$, where $[\underline{\delta}^h,\ \overline{\delta}^h]$ is given by

$$[\underline{\delta}^h,\ \overline{\delta}^h] = \Box\big(\Theta_i^*(\bar{A}_i)^{\urcorner_\downarrow(k-0)}(\tilde{A}_i)^{\urcorner_\uparrow(k-0)}\hat{\zeta}^z(0)\big) \oplus \bigoplus_{\varsigma=0}^{k-1}\Box\big(\Theta_i^*(\bar{A}_i)^{\urcorner_\downarrow[k-(\varsigma+1)]}(\tilde{A}_i)^{\urcorner_\uparrow[k-(\varsigma+1)]}B_i^{\diamond}\Omega\big),$$

with

$$[\underline{\delta}^h(0),\ \overline{\delta}^h(0)] = \Box\big(\langle 0,\ \tilde{\Theta}_i P(0)\rangle\big).$$

Proof. Given the Remark 2.4, we have

$$\begin{cases} \delta(k+1) = \tilde{\Theta}_i\tilde{A}_i z + \tilde{\Theta}_i\tilde{B}_i u, & \forall k \in \urcorner_\uparrow(k_F, k_{F+1}) \\ \delta(k+1) = \bar{\Theta}_i\bar{A}_i z + \bar{\Theta}_i\bar{B}_i u. & \forall k \in \urcorner_\downarrow(k_F, k_{F+1}) \end{cases} \tag{34}$$

Then, the error (34) is equivalent to

$$\delta(k) = \Theta_i^* \left[(\bar{A}_i)^{\urcorner_\downarrow (k-0)} (\tilde{A}_i)^{\urcorner_\uparrow (k-0)} z(0) + \sum_{\varsigma=0}^{k-1} (\bar{A}_i)^{\urcorner_\downarrow [k-(\varsigma+1)]} (\tilde{A}_i)^{\urcorner_\uparrow [k-(\varsigma+1)]} B_i^\diamond u(\varsigma) \right], \tag{35}$$

where $B_i^\diamond$ is a matrix varying with the modes, and its values are given by

$$B_i^\diamond = \begin{cases} \bar{B}_i, & \text{if } \varsigma \in \urcorner_\downarrow \\ \tilde{B}_i. & \text{if } \varsigma \in \urcorner_\uparrow \end{cases}$$

Since $z(0) \in \hat{\zeta}^z(0) = \langle 0,\ P(0) \rangle$, for $\delta(0) = \hat{\xi}(0) - \xi(0) = \tilde{\Theta}_i z(0)$, it yields

$\delta(0) \in \hat{\zeta}^h(0) = \tilde{\Theta}_i \hat{\zeta}^z(0) = \langle 0,\ \tilde{\Theta}_i P(0) \rangle.$

Thus, the zonotope $\hat{\zeta}^h(0)$ can be enclosed by following IV

$\hat{\zeta}^h(0) \subseteq [\underline{\delta}^h(0), \overline{\delta}^h(0)] = \square\big(\langle 0,\ \tilde{\Theta}_i P(0) \rangle\big).$

Substitute Eqs. (32) and (33) into Eq. (35), and the reachable set that contain Eq. (35) can be obtained by

$$\begin{aligned} \delta(k) \in \hat{\zeta}^h(k) = \Theta_i^* \Big[& (\bar{A}_i)^{\urcorner_\downarrow (k-0)} (\tilde{A}_i)^{\urcorner_\uparrow (k-0)} \hat{\zeta}^z(0) \oplus \\ & \bigoplus_{\varsigma=0}^{k-1} (\bar{A}_i)^{\urcorner_\downarrow [k-(\varsigma+1)]} (\tilde{A}_i)^{\urcorner_\uparrow [k-(\varsigma+1)]} B_i^\diamond \langle 0,\ U \rangle \Big]. \end{aligned} \tag{36}$$

From Eq. (36) and Property 2, the IH of $\hat{\zeta}^h$ can be obtained by

$$\begin{aligned} \square\big(\hat{\zeta}^h\big) = {} & \square\big(\Theta_i^* (\bar{A}_i)^{\urcorner_\downarrow (k-0)} (\tilde{A}_i)^{\urcorner_\uparrow (k-0)} \hat{\zeta}^z(0)\big) \oplus \\ & \bigoplus_{\varsigma=0}^{k-1} \square\big(\Theta_i^* (\bar{A}_i)^{\urcorner_\downarrow [k-(\varsigma+1)]} (\tilde{A}_i)^{\urcorner_\uparrow [k-(\varsigma+1)]} B_i^\diamond \Omega\big). \end{aligned} \tag{37}$$

Since $\delta \in \hat{\zeta}^h \subseteq \square\big(\hat{\zeta}^h\big)$, we get

$[\underline{\delta}^h, \overline{\delta}^h] = \square\big(\hat{\zeta}^h\big).$

The following iterative algorithm can be used to implement Theorem 3.2. $\square$

4. Comparisons and relationships between the RA technique and the zonotope method

In this section, comparisons and relationships between the RA technique and zonotope-based method are discussed in theory.

Theorem 4.1. *Given observers (30) and (31), with the same initial conditions* $\underline{\xi}^h(0) = \underline{\xi}^z(0)$, $\overline{\xi}^h(0) = \overline{\xi}^z(0)$, *the following inequalities hold*

$$\begin{cases} \overline{\xi}^z \geq \overline{\xi}^h, \\ \underline{\xi}^z \leq \underline{\xi}^h, \end{cases}$$

where $\overline{\xi}^z$, $\underline{\xi}^z$, $\overline{\xi}^h$ *and* $\underline{\xi}^h$ *are obtained by Eqs. (30) and (31).*

Proof. Given the formula (29), it is derived that

$$\begin{aligned}\hat{\xi}^z(k+1) &= \langle 0, P(k+1)\rangle \\ &= A_i^* \odot \langle 0, \hat{P}(k)\rangle \oplus B_i^* \odot \langle 0, U\rangle.\end{aligned} \tag{38}$$

Due to $\langle 0, P(k)\rangle \subseteq \langle 0, \hat{P}(k)\rangle$, we have

$$\hat{\xi}^z(k+1) \supseteq A_i^* \odot \langle 0, P(k)\rangle \oplus B_i^* \odot \langle 0, U\rangle. \tag{39}$$

Repeating Eqs. (38) and (39), it can be derived that

$$\begin{aligned}\hat{\xi}^z(k) \supseteq\ & (\bar{A}_i)^{\urcorner_{\downarrow}(k-0)}(\tilde{A}_i)^{\urcorner_{\uparrow}(k-0)}\hat{\xi}^z(0) \oplus \\ & \bigoplus_{\varsigma=0}^{k-1}(\bar{A}_i)^{\urcorner_{\downarrow}[k-(\varsigma+1)]}(\tilde{A}_i)^{\urcorner_{\uparrow}[k-(\varsigma+1)]}B_i^{\diamond}\Omega,\end{aligned}$$

and

$$\begin{aligned}\square\big(\Theta_i^*\hat{\xi}^z\big) \supseteq\ & \square\big(\Theta_i^*(\bar{A}_i)^{\urcorner_{\downarrow}(k-0)}(\tilde{A}_i)^{\urcorner_{\uparrow}(k-0)}\hat{\xi}^z(0)\big) \oplus \\ & \bigoplus_{\varsigma=0}^{k-1}\square\big(\Theta_i^*(\bar{A}_i)^{\urcorner_{\downarrow}[k-(\varsigma+1)]}(\tilde{A}_i)^{\urcorner_{\uparrow}[k-(\varsigma+1)]}B_i^{\diamond}\Omega\big).\end{aligned} \tag{40}$$

Based on Eqs. (37) and (40), we have

$$\square(\Theta_i^*\hat{\xi}^z) \supseteq \square(\hat{\xi}^h). \tag{41}$$

By Remark 3.4 and Theorem 3.2, we have $\square(\Theta_i^*\hat{\xi}^z) = [\underline{\delta}^z, \overline{\delta}^z]$ and $\square(\hat{\xi}^h) = [\underline{\delta}^h, \overline{\delta}^h]$. Then, the formula (41) implies

$$\begin{cases}\overline{\delta}^z \geq \overline{\delta}^h, \\ \underline{\delta}^z \leq \underline{\delta}^h.\end{cases}$$

By Eqs. (30) and (31), it is easy to see that

$$\begin{cases}\overline{\xi}^z \geq \overline{\xi}^h, \\ \underline{\xi}^z \leq \underline{\xi}^h.\ \square\end{cases}$$

Remark 4.1. It is clear from the proof of Theorem 4.1 that the reduced-order operation in zonotope algorithm is avoided by Algorithm 1 and the accuracy of the FIO is further improved.

Remark 4.2. As shown in Alamo et al. [21], the reduced-order operation is a relatively complicated computation process. Whereas, Algorithm 1 simplifies the complexity of the zonotope algorithm to a certain extent. In addition, the structure of the error system (35) in Algorithm 1 also avoids the impossibility of computation caused by the increase of zonotope order.

Remark 4.3. Compared with the previous work in Huang et al. [27], the zonotopic SME method in Huang et al. [27] is extended to FIO and this observer structure greatly reduces the design complexity of the observer. In addition, the work in Huang et al. [27]only considered the completely asynchronous case, this paper further considers the case that the switching signal of the system is partly asynchronous with the switching signal of the observer, which is a more general case of AS in practice.

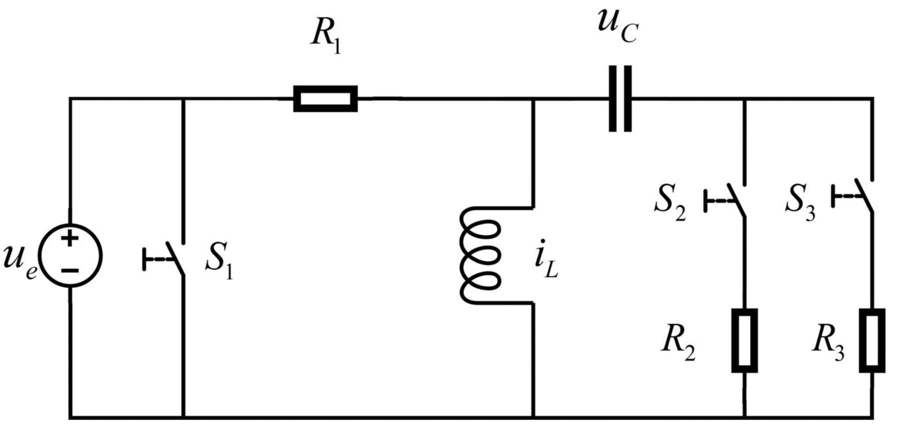

Fig. 3. Diagram of a circuit system .

Remark 4.4. In this paper, we consider the external disturbance $\omega(k)$ with H_∞ performance, i.e., it requires the energy performance of the system disturbance on the whole time domain, and $\sum_{k=0}^{\infty} \omega^T(k)\omega(k) < \eta$, for some constant $\eta > 0$. It is obvious that if one signal with H_∞ performance also behaves L_∞ performance, otherwise, it does not hold. If we consider disturbance $\omega(k)$ with L_∞ performance, i.e., $\omega^T(k)\omega(k) < c$, for some constant $c > 0$, the first step is to find an L_∞ functional observer for the system (1) and the second step is the same as that in this paper.

5. Simulation

Consider the circuit system in previous work [27], and the circuit diagram is depicted in Fig. 3. When the capacitor discharges, the dynamic of plant is described by

$$\begin{cases} \dfrac{du_C(t)}{dt} = -\dfrac{1}{(R_1 + R_2S(t) + R_3(1 - S(t)))C} u_C(t) \\ \qquad -\dfrac{R_1}{(R_1 + R_2S(t) + R_3(1 - S(t)))C} i_L(t), \\ \dfrac{di_L(t)}{dt} = \dfrac{R_1}{(R_1 + R_2S(t) + R_3(1 - S(t)))L} u_C(t) \\ \qquad -\dfrac{R_1(R_2S(t) + R_3(1 - S(t))}{(R_1 + R_2S(t) + R_3(1 - S(t)))L} i_L(t), \end{cases}$$

where S_1, S_2 and S_3 are the switches. Denote

$$S(t) = S_2(t) = \begin{cases} 0, & Switch \quad on \\ 1, & Switch \quad off \end{cases}$$

and $S_2(t) + S_3(t) = 1$. i_L stands for the inductance current and u_C denotes the capacitance voltage. Here, the state vector is $x = [u_C, i_L]^T$ and the output is the voltage of R_2 or R_3, that is,

$$y(t) = -\frac{R_2S(t) + R_3(1 - S(t))}{R_1 + R_2S(t) + R_3(1 - S(t))} u_C(t)$$

$$-\frac{R_1(R_2S(t)+R_3(1-S(t))}{R_1+R_2S(t)+R_3(1-S(t))}i_L(t),$$

Denote the disturbance by $B_i\omega(k)$, where

$$B_1=\begin{bmatrix}0.02\\0.09\end{bmatrix},\ B_2=\begin{bmatrix}0.05\\0.07\end{bmatrix},$$

In addition, $D_if(k)$ is supposed to be the observation noise in the output, where $D_1=0.03,\ D_2=0.06$. Both $\omega(k)$ and $f(k)$ are unknown and bounded, and their bounds are $\underline{\omega}=-1$, $\overline{\omega}=1$, $\underline{f}=-1$ and $\overline{f}=1$ respectively. In the simulation, $L=0.8H,\quad C=0.5F,\quad R_1=1\Omega$, $R_2=2\Omega$, and $R_3=3\Omega$. Then, by the explicit Euler method, the following DSS can be obtained:

$$\begin{cases}x(k+1)=A_ix(k)+B_i\omega(k),\\ y(k)=C_ix(k)+D_if(k),\end{cases}$$

where

$$A_1=\begin{bmatrix}0.3333 & -0.6667\\0.4167 & 0.1667\end{bmatrix},\ A_2=\begin{bmatrix}0.5 & -0.5\\0.3125 & 0.0625\end{bmatrix},$$

$$C_1=[-0.6667\quad -0.6667],\ C_2=[-0.75]^{-0.75}],$$

$x(k)=[u_C(k),i_L(k)]^T$. Thus, the output $y(k)$ is the combination of the voltage $u_C(k)$ and current $i_L(k)$ and it is also the estimation object. The parameters of F_i are defined as

$$F_1=C_1=\begin{bmatrix}-0.6667 & -0.6667\end{bmatrix},$$
$$F_2=C_2=\begin{bmatrix}-0.75 & -0.75\end{bmatrix}.$$

The same initial conditions are given, namely,

$$P(0)=\begin{bmatrix}1.5&0&0&0\\0&1.5&0&0\\0&0&1.5&0\\0&0&0&1.5\end{bmatrix},$$

$$[\underline{\delta}^z(0),\bar{\delta}^z(0)]=[\underline{\delta}^h(0),\bar{\delta}^h(0)]=\square(\langle 0,\ \tilde{\Theta}_1P(0)\rangle),$$

and $\hat{\xi}(0)=-5.25$. Let $\pi=1.05$, $\alpha=0.1$, $\beta=0.05$ and $\urcorner_M=1$, by solving Eqs (9)–(12), then

$$L_1=\begin{bmatrix}0.077\\-0.9235\end{bmatrix},\ L_2=\begin{bmatrix}-0.1625\\-1.533\end{bmatrix},\ \gamma=0.05,\ \tau^*\geq 1.93.$$

The switching sequences of the circuit system and the observer are shown in Fig. 4. The simulation results are illustrated in Fig. 5. As shown, under the same conditions, the FIO designed by RA technique is better than that designed by the method in Huang et al. [27]. It sufficiently illustrates the correctness of theoretical analysis in Section 3.

Remark 5.1. As illustrated in Fig. 4, the switching sequence of the circuit system is partly synchronous and asynchronous with the switching sequence of the observer. The total switching times of the original system and observer are the same. By a direct computation, the ADT of the switching sequence is about 2.85 and it satisfies the condition $\tau^*\geq 1.93$.

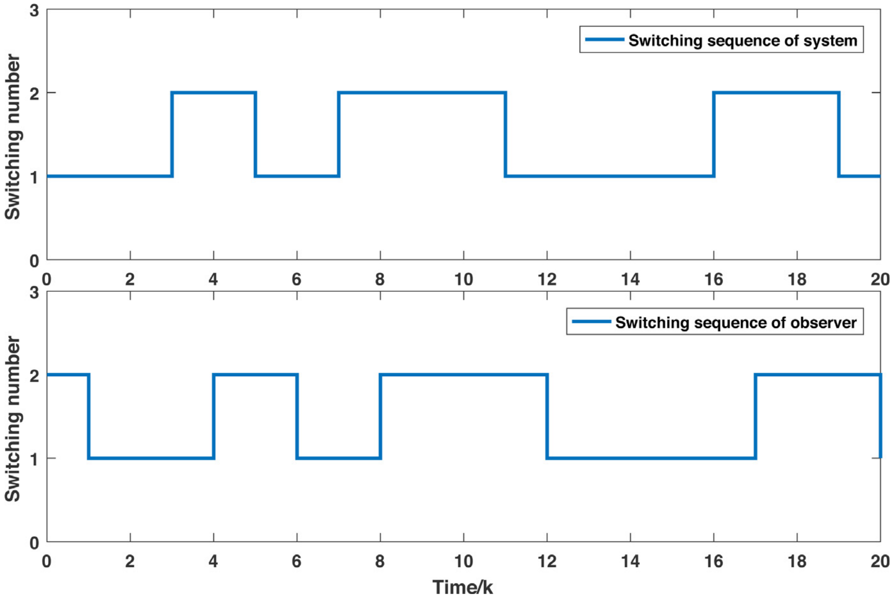

Fig. 4. Time response of the switching sequence.

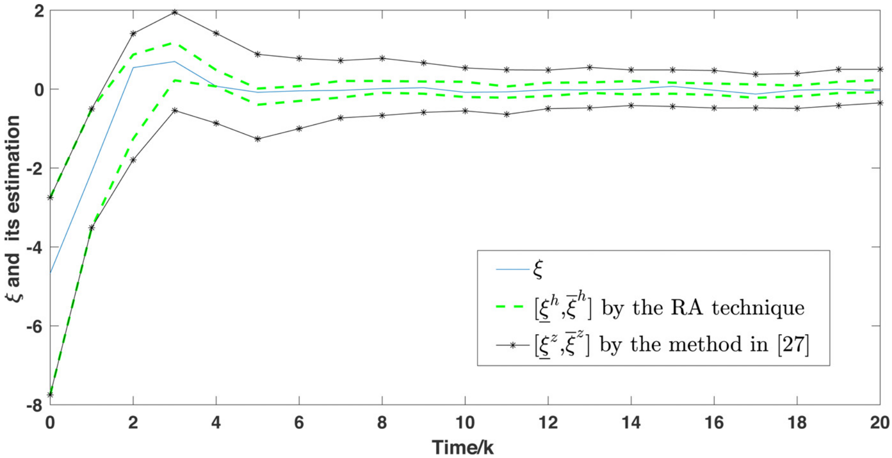

Fig. 5. Evolutions of ξ, $\underline{\xi}^h$, $\overline{\xi}^h$, $\underline{\xi}^z$, $\overline{\xi}^z$.

Remark 5.2. From the practical perspective, the estimation object is ξ. The accurate interval of ξ may be applied in the feedback control or fault estimation problem. By using the proposed method in this paper, when the convergence time is about 7.5, the interval of upper and lower error is about $[-0.21, 0.21]$, while using the method in Huang et al. [27], the interval of upper and lower error is about $[-0.64, 0.49]$ when the convergence time is about 10.6. Thus, we can use the suggested method in this paper to obtain the estimated interval for ξ.

6. Conclusion

A novel estimation method was proposed to design FIO for DSSs under AS in this paper. By allowing the LF to increase during the running of system, an optimal H_∞ FO was constructed, and a WDA level γ was obtained. Based on the designed FO, the boundaries of the estimated object were recovered by the RA technique. This new type of observer structure does not require the error systems to be cooperative, so the design constraints of observers are relaxed. Moreover, compared with the zonotope-based method, the proposed method avoids the reduction-order operation and effectively improves the estimation accuracy of FIO. Finally, an application example was given to illustrate the effectiveness of our results. We will focus on the investigation of the IO design for nonlinear switched systems in the nearly future.

Declaration of Competing Interest

The authors declare that they have no known competing financial interests or personal relationships that could have appeared to influence the work reported in this paper.

CRediT authorship contribution statement

Jun Huang: Methodology, Software, Writing – original draft. **Haochi Che:** Conceptualization, Validation, Writing – review & editing. **Hieu Trinh:** Visualization. **Xudong Zhao:** Supervision. **Yueyuan Zhang:** Project administration, Writing – review & editing.

Acknowledgments

This work is supported by the Natural Science Foundation of Jiangsu Province of China (BK2021-1309) and the Open Fund for Jiangsu Key Laboratory of Advanced Manufacturing Technology (HGAMTL-2101).

References

[1] M. Zhang, J. Huang, G. Zong, X. Zhao, Y. Zhang, Observer design for semi-Markov jump systems with incremental quadratic constraints, J. Frankl. Inst. 358 (10) (2021) 5599–5622.
[2] J. Fu, T. Chai, Y. Jin, C. Su, Fault-tolerant control of a class of switched nonlinear systems with structural uncertainties, IEEE Trans. Circuits Syst. II 63 (2) (2016) 201–205.
[3] Y. Chang, P. Zhou, B. Niu, H. Wang, N. Xu, M.O. Alassafi, A.M. Ahmad, Switched-observer-based adaptive output-feedback control design with unknown gain for pure-feedback switched nonlinear systems via average dwell time, Int. J. Syst. Sci. 52 (9) (2021) 1731–1745.
[4] B. Hu, G. Zhai, A. Michel, Common quadratic Lyapunov-like functions with associated switching regions for two unstable second-order LTI systems, Int. J. Control 75 (14) (2002) 1127–1135.
[5] X. Liu, Stability analysis of switched positive systems: aswitched linear copositive Lyapunov function method, IEEE Trans. Circuits Syst. II 56 (5) (2009) 414–418.
[6] H. Zhang, H. Wang, B. Niu, L. Zhang, A. Ahmad, Sliding-Mode Surface-Based Adaptive Actor-Critic Optimal Control for Switched Nonlinear Systems with Average Dwell Time, Inf. Sci. 580 (2021) 756–774.
[7] W. Xiang, J. Xiao, M. Iqbal, Robust observer design for nonlinear uncertain switched systems under asynchronous switching, Nonlinear Anal. 6 (1) (2012) 754–773.
[8] H. Lin, S. Sun, Optimal sequential estimation for asynchronous sampling discrete time systems, IEEE Trans. Signal Process. 68 (2020) 6117–6127.
[9] Z. Li, L. Long, Global stabilization of switched feedforward nonlinear time-delay systems under asynchronous switching, IEEE Trans. Circuits Syst. I 67 (2) (2020) 711–724.

[10] S. Shi, Z. Fei, M. Dai, Asynchronously bounded filtering for discrete-time switched positive systems, Nonlinear Anal. 44 (2022) 101121.

[11] L. Zhang, P. Shi, Stability, l_2-gain and asynchronous H_∞ control of discrete-time switched systems with average dwell time, IEEE Trans. Autom. Control 54 (9) (2009) 2192–2199.

[12] G. Zhai, B. Hu, K. Yasuda, A. Michel, Disturbance attenuation properties of time-controlled switched systems, J. Frankl. Inst. 338 (7) (2001) 765–779.

[13] J. Gouzé, A. Rapaport, M. Hadj-Sadok, Interval observers for uncertain biological systems, Ecol. Model. 133 (1–2) (2000) 45–56.

[14] G. Marouani, T.N. Dinh, T. Raïssi, X. Wang, H. Messaoud, Unknown input interval observers for discrete-time linear switched systems, Eur. J. Control 59 (2021) 165–174.

[15] Y. Garbouj, T.N. Dinh, T. Raïssi, T. Zouari, M. Ksouri, Optimal interval observer for switched Takagi–Sugeno systems: an application to interval fault estimation, IEEE Trans. Fuzzy Syst. 29 (8) (2020) 2296–2309.

[16] C. Combastel, Zonotopes and Kalman observers: gain optimality under distinct uncertainty paradigms and robust convergence, Automatica 55 (2015) 265–273.

[17] Z. Wang, C. Lim, Y. Shen, Interval observer design for uncertain discrete-time linear systems, Syst. Control Lett. 116 (2018) 41–46.

[18] Z. Wang, P. Shi, C. Lim, $H-/H_\infty$ fault detection observer in finite frequency domain for linear parameter-varying descriptor systems, Automatica 86 (2017) 38–45.

[19] S. Liu, Z. Wang, L. Wang, G. Wei, Recursive set-membership state estimation over a flexray network, IEEE Trans. Syst., Man, Cybern. (2021), doi:10.1109/TSMC.2021.3071390. to be published

[20] F. Chernousko, Ellipsoidal state estimation for dynamical systems, Nonlinear Anal. 63 (5) (2005) 872–879.

[21] T. Alamo, J. Bravo, E. Camacho, Guaranteed state estimation by zonotopes, Automatica 41 (6) (2005) 1035–1043.

[22] J. Li, Z. Wang, Y. Shen, M. Rodrigues, Zonotopic fault detection observer for linear parameter varying descriptor systems, Int. J. Robust Nonlinear Control 29 (11) (2019) 3426–3445.

[23] J. Huang, X. Ma, H. Che, Z. Han, Further result on interval observer design for discrete-time switched systems and application to circuit systems, IEEE Trans. Circuits Syst. II 67 (11) (2020) 2542–2546.

[24] X. Li, W. Zhang, D. Lu, Zonotopic fault interval estimation for discrete-time Markovin jump systems with generally bounded transition probabilities, J. Frankl. Inst. 358 (3) (2021) 2138–2160.

[25] H. Zhang, J. Huang, H. Che, Z. Han, Optimal interval observer for discrete-time switched systems, IEEE Trans. Circuits Syst. II 69 (3) (2022) 1233–1237.

[26] J. Huang, H. Che, T. Raïssi, Z. Wang, Functional interval observer for discrete-time switched descriptor systems, IEEE Trans. Autom. Control (2021), doi:10.1109/TAC.2021.3079193. to be published

[27] J. Huang, X. Ma, X. Zhao, H. Che, L. Chen, Interval observer design method for asynchronous switched systems, IET Control Theory Appl. 14 (8) (2020) 1082–1090.

[28] W. Kühn, Rigorously computed orbits of dynamical systems without the wrapping effect, Computing 61 (1) (1998) 47–67.

[29] W. Tang, Z. Wang, Y. Wang, T. Raïssi, Y. Shen, Interval estimation methods for discrete-time linear time-invariant systems, IEEE Trans. Autom. Control 64 (11) (2019) 4717–4724.

[30] H. Trinh, T. Fernando, Functional Observers for Dynamical Systems, Springer, 2011.

[31] K. Emami, T. Fernando, B. Nener, H. Trinh, Y. Zhang, A functional observer based fault detection technique for dynamical systems, J. Frankl. Inst. 352 (5) (2015) 2113–2128.

[32] T. Fernando, H. Trinh, L. Jennings, Functional observability and the design of minimum order linear functional observers, IEEE Trans. Autom. Control 55 (5) (2010) 1268–1273.

[33] L. Jennings, T. Fernando, H. Trinh, Existence conditions for functional observability from an eigenspace perspective, IEEE Trans. Autom. Control 56 (12) (2011) 2957–2961.

[34] D. Gu, L. Liu, G. Duan, Functional interval observer for the linear systems with disturbances, IET Control Theory Appl. 12 (18) (2018) 2562–2568.

[35] H. Che, J. Huang, X. Zhao, X. Ma, N. Xu, Functional interval observer for discrete-time systems with disturbances, Appl. Math. Comput. 383 (2020). Article, 125352

[36] D. Huong, V. Huynh, H. Trinh, Distributed functional interval observers for nonlinear interconnected systems with time-delays and additive disturbances, IEEE Syst. J. 15 (1) (2021) 411–422.

[37] S. Boyd, L. Ghaoui, E. Feron, Linear Matrix Inequalities in System and Control Theory, SIAM Press, New York, 1994.